

## Experimental determination of the energy barrier for the $\text{Li}_{26}^{2+}$ cluster

C. Bréchnignac, Ph. Cahuzac, M. de Frutos, P. Garnier, and N. Kebaili

Laboratoire Aimé Cotton, CNRS II, Campus d'Orsay, Bâtiment 505, 91405 Orsay cedex, France

(Received 16 May 1995)

Photoinduced Coulombic fission of doubly charged lithium-atom clusters is observed for cluster sizes around the critical size of stability. The absolute value of the outer part of the Coulombic barrier is deduced from kinetic-energy-release measurements. The inner part is obtained from unimolecular decay. Such analysis provides a complete characterization of the energetics of the fissioning system.

Experimental studies of dissociation processes of doubly charged single "s" electron-atom clusters have been the subject of recent publications.<sup>1-4</sup> These finite fermionic systems exhibit Coulombic fission into two singly charged fragments. Detailed studies on alkali-metal-atom clusters have shown that fission predominates at small sizes, whereas evaporation of a neutral monomer (or dimer) prevails at large size.<sup>3,4</sup> The limit between both domains is given by the so-called critical size of stability  $n_c$ .<sup>5</sup> Below this size, the repulsive Coulombic forces overcome the binding forces and Coulombic fission prevails. Above  $n_c$ , neutral evaporation is the preferential decay channel. More precisely the analysis of the energetics suggests that around  $n_c$ , the fission barrier  $B_{n,p}^{2+}$  should be comparable to the dissociation energy for the evaporation of a neutral monomer (or dimer)  $D_{n,1(2)}^{2+}$  (Fig. 1). For  $\text{Li}_n^{2+}$  clusters we have found  $n_c=25$ . According to that scheme, the fragmentation channels simultaneously exhibit fission and evaporation products due to the competition between both processes.<sup>3,4</sup>

Since the potential-energy barrier governs the dynamics of the fission process, it is of primary importance to determine its absolute value. Up to now the inner part of the Coulombic barrier has been obtained by studying the unimolecular decay of doubly charged alkali-atom clusters in the critical size range.<sup>4</sup> On the other hand, the outer part of the Coulombic barrier (i.e., for a fission process) has been determined from the kinetic energy released from the fission of unstable doubly charged species for sizes somewhat smaller than  $n_c$ . In this paper we emphasize an experimental procedure allowing the determination of both parts of the Coulombic barrier of clusters in the vicinity of the critical size. These results, in their whole, provide a complete determination of the energetics of Coulombic fission.

The experimental setup has already been described in detail.<sup>4</sup> Briefly, a neutral distribution of clusters produced by a gas-aggregation source<sup>6,7</sup> is ionized by a pulsed UV laser source and accelerated at 4.5 kV typically. Cluster ions enter a tandem time-of-flight mass spectrometer where they spatially resolve into mass packets. In the first time of flight a couple of deflecting plates selects a given size of parent ions. For those undergoing unimolecular decay during their flight, a retarding potential followed by the second time of flight allows us to separate residual parent and unimolecular fragments in time.<sup>4</sup> As an example, Fig. 2 shows the unimolecular fragmentation spectrum of  $\text{Li}_{26}^{2+}$  and  $\text{Li}_{13}^+$ . Peaks arriving at times earlier than the parent arrival time are due to the highest fragments of the fission process. Peaks arriving at

later times are the ionic fragments from neutral evaporation. It can be noted that both evaporation and Coulombic fission contribute to the dissociation of  $\text{Li}_{26}^{2+}$ . Concerning its fission into two singly charged fragments, the main channel leads to  $\text{Li}_{23}^+$  as the highest fragment, and consequently  $\text{Li}_3^+$  must be the lightest one. In order to observe the light fission product the experimental setup is modified as follows. The retarding potential is replaced by a decelerating/accelerating multiplate system. In between the central plates the selected parents are fired with a second laser source, a pulsed ArF excimer laser oscillating at  $h\nu=6.42$  eV crossing the cluster beam at right angles.<sup>8</sup> The photoexcitation of  $\text{Li}_n^{2+}$  at a photon energy below its ionization threshold promotes a fast heating of the parent, which fragmentates during its residence time in the interaction region. The resulting products are mass separated in the second time of flight.

As an example, Fig. 3 shows fragmentation spectra observed under various laser fluences for the doubly charged lithium cluster  $\text{Li}_{47}^{2+}$  far above the critical size  $n_c=25$ . At a low laser fluence one observes a sequence of doubly charged fragments  $\text{Li}_x^{2+}$  resulting from the photoevaporation of the parent in a size domain where the neutral evaporation is the dominant process. Each step of the sequence corresponds to the photoevaporation of five monomers following the photoabsorption of one photon at  $h\nu=6.42$  eV. This leads to an averaged dissociation energy (in the vicinity of  $n=33$ )  $D_{n,1}^{2+}\approx 1.28$  eV, a value which is comparable to the dissociation energy of the corresponding singly charged cluster  $D_{n,1}^+=1.22$  eV obtained from previous experiments.<sup>9</sup> The production of  $\text{Li}_x^{2+}$  stops in the size range of  $x\approx n_c$ , for which the fission barrier becomes smaller than the dissocia-

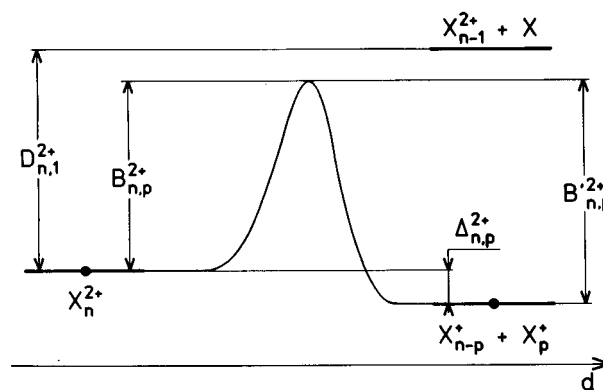


FIG. 1. Energetics of the fragmentation pathways for a doubly charged parent  $X_n^{2+}$ .

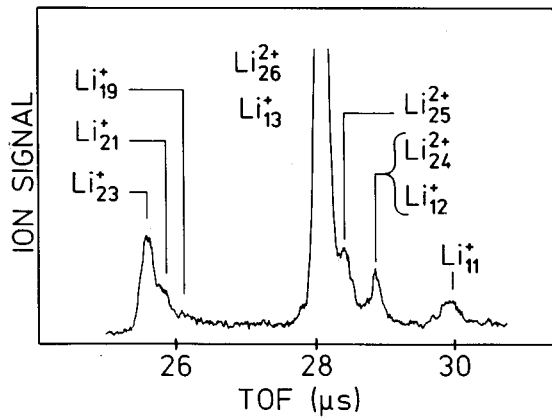


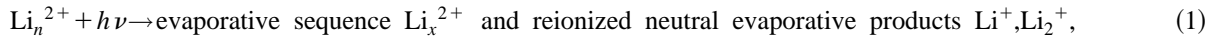
FIG. 2. Fragmentation spectrum of a selected charge/size ratio  $\text{Li}_{26}^{2+}$  and  $\text{Li}_{13}^{+}$  showing the evaporative products and the fission products in a unimolecular dissociation experiment.

tion energy  $B_{n,p}^{2+} < D_{n,1}^{2+}$ . For lithium clusters the corresponding size is  $x=26$ . Below this size fission becomes the dominant fragmentation process. As expected from the unimolecular dissociation experiment,  $\text{Li}_3^{+}$  ( $p=3$  channel) is

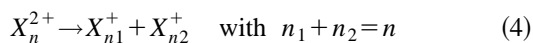
clearly observed as the most probable lightest fission fragment.

At a medium laser fluence the truncated  $\text{Li}_x^{2+}$  series is more visible. The neutral evaporative products  $\text{Li}$  and  $\text{Li}_2$  are ionized at  $h\nu=6.42$  eV and produce the  $\text{Li}^{+}$  and  $\text{Li}_2^{+}$  ion peaks. The apparent stopping size of the series is  $x=28$ . This is the closest approach from the critical size  $n=26$  allowed by the evaporative sequence: the fragment  $\text{Li}_{28}^{2+}$  is obtained after four successive sequences of photoabsorption and evaporation. The next one would produce the  $\text{Li}_{23}^{2+}$  fragment, but the quenching of the evaporative sequence by the fission process below the size  $n=26$  hinders us from reaching this fragment. The heavy fission fragment  $\text{Li}_{23}^{2+}$  still contains an excess of internal energy, and mostly decomposes. The residual weak signal cannot be discriminated from the large superimposed ion parent peak. Actually the existence of this heavy fission fragment is indirectly revealed at high laser fluence. A series of  $\text{Li}_p^{+}$  peaks appears which can be attributed to the photoevaporation of  $\text{Li}_{23}^{2+}$  following the absorption of several photons.

A summary of the sequential dissociation pathways is given as follows:



To ensure this interpretation we have measured the kinetic energy released during the fission process. By choosing a convenient voltage  $V$  of the decelerating/accelerating plates, our setup offers the advantage of being sensitive to the recoil velocity of the fragments.<sup>10</sup> Actually the kinetic-energy release for the Coulombic fission process induces a recoil velocity of the fragments which is measured by time dispersion in the second part of the time of flight. The inset of the upper trace in Fig. 3 shows the trimer ion signal at a low laser fluence and at a small value of  $V$ . The splitting of the trimer peak characterizes the recoil effect, taking into account that the small acceptance angle of our device allows us to detect only the fragments which propagate relatively close to the drift tube axis. At a high laser fluence this splitting is still visible as shoulders superimposed on the single-ion peak due to the thermal evaporative process (3). The kinetic energy of a fragment of mass  $m_{n1}$  in the fission process



is given by

$$\xi m_{n1}(\text{eV}) = \left( \frac{\Delta t}{1.444L} \right)^2 \frac{m_n m_{n1}}{U_0 - V} \left( \frac{V}{m_{n1}} + \frac{U_0 - V}{m_n} \right)^3, \quad (5)$$

where  $\Delta t$  is the time splitting,  $L$  the length of the second drift tube,  $U_0$  the initial acceleration energy of the parent of mass  $m_n$  ( $m_n$ , and  $m_{n1}$  in a.u.;  $U_0$  and volts in V, and  $L$  in cm). The total kinetic energy involved in (4) is

$$\xi = \xi m_{n1} + \xi m_{n2} = \xi m_{n1} \left( 1 + \frac{m_{n2}}{m_{n1}} \right). \quad (6)$$

This is nothing else but the outer part of the Coulombic barrier associated with (4), provided that there is no transfer between the potential energy and the vibrational internal energy of the fragments.

The validity of our interpretation summarized in processes (1)–(3) is also ensured through our measurements performed in the size range  $n=26$ –53. As shown in Table I, one obtains the same value for  $\xi_{3+}$  whatever the starting parent is. This would not be the case if the fission observed comes directly from the selected parent itself. Then we can conclude that we have measured the outer part of the potential energy barrier, i.e., the fission barrier  $B_{n,3}'^{2+}$  for  $n=26$  only:

$$B_{26,3}'^{2+} = 1.19 \pm 0.1 \text{ eV},$$

The unimolecular dissociation experiment for the same size gives the inner part of the potential-energy barrier, i.e. the fission barrier  $B_n^{2+}$ , by comparing the rates of fission and evaporation processes,<sup>4</sup>

$$B_{26,3}^{2+} = 1.10 \pm 0.08 \text{ eV}.$$

As the energy balance for process (4), one deduces

$$B_{26,3}^{2+} - B_{26,3}'^{2+} = -0.09 \pm 0.2 \text{ eV}.$$

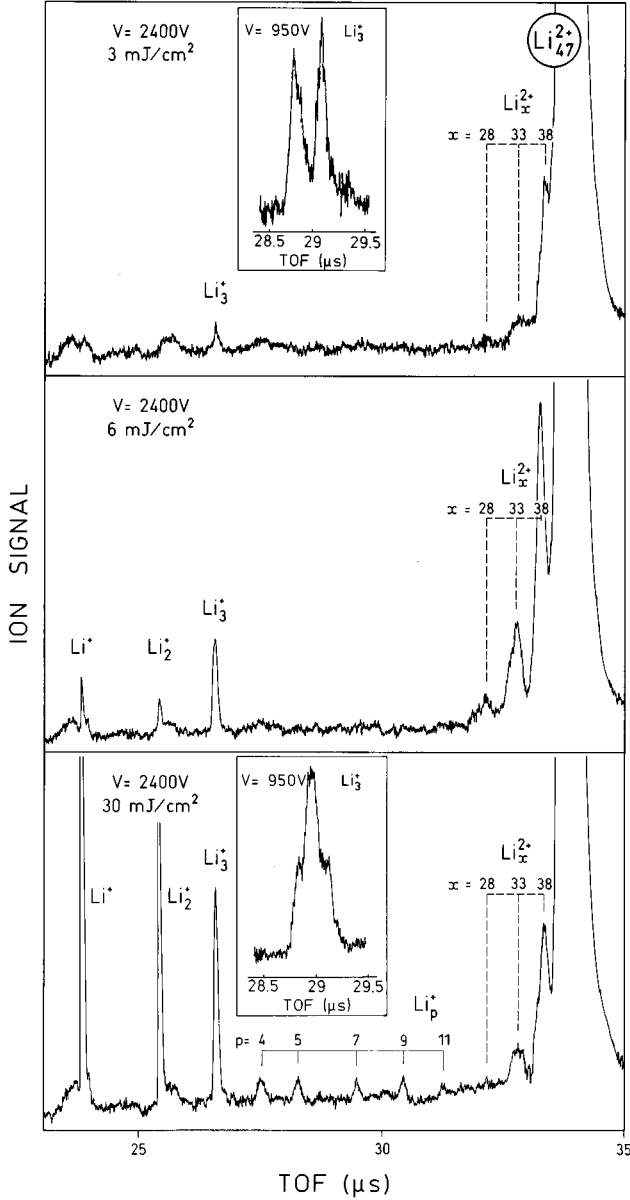


FIG. 3. Fragmentation spectra of  $\text{Li}_{47}^{2+}$  following a photoexcitation at  $h\nu=6.42$  eV in a photoinduced dissociation experiment. Three levels of laser fluence have been used and two different values of the retarding potential  $V$ .

This value can be compared to the one obtained from the total energies of the parent and the fragments. This has been achieved from our measured dissociation energies, atomization energies, and ionization potentials as previously reported,<sup>4</sup> leading to

$$\Delta_{26,3}^{2+} = -0.06 \pm 0.2 \text{ eV},$$

TABLE I. Kinetic energy released by the light fragment  $\text{Li}_3^+$  in the fission process  $\text{Li}_n^{2+} \rightarrow \text{Li}_{n-3}^+ + \text{Li}_3^+$  for some sizes of selected parent.

$n$	26	27	29	30	31	37	39	53
$\xi_{3^+}$ (eV)	0.93	1.08	1.14	1.05	1.06	1.14	1.02	1.01

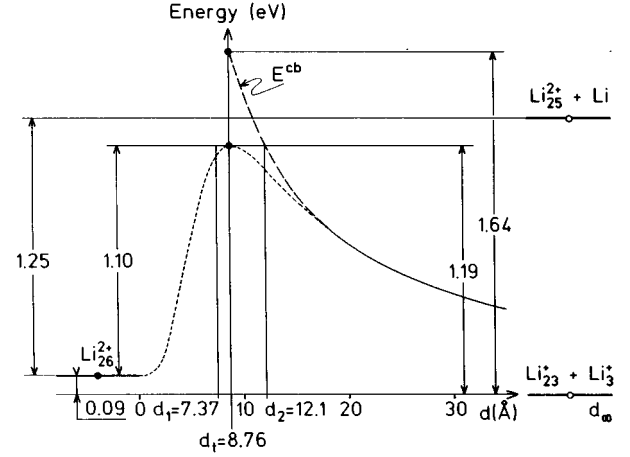


FIG. 4. Experimental values of the energetics parameters for the  $\text{Li}_{26}^{2+} \rightarrow \text{Li}_{23}^+ + \text{Li}_3^+$  process. The dashed curve: pure Coulombic energy  $E^{\text{cb}}$ .

The good agreement between the two determinations of the energy balance, within the experimental uncertainties, strengthens our assumption of no noticeable conversion of the potential energy into the internal energy of the system.

It is then possible to go further and to discuss on the shape of the potential-energy barrier. This can be done in the two-dimensional potential-energy diagram  $E(d)$ , where  $d$  is the center-of-mass distance between the two fragments  $\text{Li}_{23}^+$  and  $\text{Li}_3^+$ . The asymptotic value and the maximum of the barrier are deduced from the values of  $B_{26,3}^{2+}$  and  $B_{26,3}^{\prime 2+}$ . At large  $d$ , i.e., for well-separated fragments, the asymptotic behavior of the barrier can be well described by the pure Coulombic repulsive curve of two point charges:

$$E^{\text{cb}} \text{ (eV)} = \frac{14.4}{d \text{ (Å)}}. \quad (7)$$

At a moderate value of  $d$ ,  $E^{\text{cb}}$  constitutes an upper limit for the fusion barrier (Fig. 4). It follows that the distance  $d_{\text{max}}$  between the fragments at the maximum of the barrier has an upper limit determined by

$$B_{26,3}^{\prime 2+} = E^{\text{cb}},$$

giving

$$d_{\text{max}} \leq 12.1 \text{ Å}.$$

The lower limit is given by the contact distance between the ionic cores of the fragments, assumed to be spherical:

$$d_{\max} \geq 7.37 \text{ \AA}.$$

In between these two limits lies the contact distance  $d_c$  of the electronic clouds of the fragments:

$$d_c = 8.76 \text{ \AA}.$$

The value of  $E^{\text{cb}}$  at this contact distance is often considered representative of the maximum of the energy barrier.<sup>3,11</sup> In our case this obviously would lead to a strongly overesti-

mated value of the barrier, as compared with experimental results.

Although we are blind dealing with the precise shape of the barrier at its maximum, the above considerations are in favor of a strongly deformed system in the distance domain of the maximum of the barrier, implying preformed fission fragments. This is in agreement with recent theoretical findings, and might be suitable for a test of refined calculations on the dynamics of such systems.<sup>10,12</sup>

---

<sup>1</sup>I. Katakuse, H. Iko, and T. Ichihara, *Int. J. Mass. Spectrom. Ion Process.* **97**, 47 (1990).

<sup>2</sup>W. A. Saunders, *Phys. Rev. Lett.* **64**, 3046 (1990).

<sup>3</sup>C. Br  chignac, Ph. Cahuzac, F. Carlier, J. Leygnier, and A. Sarfati, *Phys. Rev. B* **44**, 11 386 (1991).

<sup>4</sup>C. Br  chignac, Ph. Cahuzac, F. Carlier, and M. de Frutos, *Phys. Rev. B* **49**, 2825 (1994).

<sup>5</sup>K. Sattler, J. M  hlbach, O. Echt, P. Pfau, and E. Recknagel, *Phys. Rev. Lett.* **47**, 160 (1981).

<sup>6</sup>K. Sattler, J. M  hlbach, and E. Recknagel, *Phys. Rev. Lett.* **45**, 821 (1980).

<sup>7</sup>F. Frank, W. Schultze, B. Tesche, J. Urban, and B. Winter, *Surf. Sci.* **156**, 90 (1985).

<sup>8</sup>C. Br  chignac, Ph. Cahuzac, F. Carlier, M. de Frutos, and J. Leygnier, *J. Chem. Phys.* **93**, 7449 (1990).

<sup>9</sup>C. Br  chignac, H. Busch, Ph. Cahuzac, and J. Leygnier, *J. Chem. Phys.* **101**, 6992 (1994).

<sup>10</sup>C. Br  chignac, Ph. Cahuzac, F. Carlier, M. de Frutos, R. N. Barnett, and U. Landman, *Phys. Rev. Lett.* **72**, 1636 (1994).

<sup>11</sup>F. Garcias, J. A. Alonso, J. M. Lopez, and M. Barranco, *Phys. Rev. B* **43**, 9459 (1991).

<sup>12</sup>R. N. Barnett, U. Landman, and G. Rajagopal, *Phys. Rev. Lett.* **67**, 3058 (1991).